Stress–Strain Analysis of Heavy Haul Rail Track with Steel Slag Ballast by Laboratory Tests and Numerical Simulations

Bruno Guimarães Delgado, António Viana da Fonseca, and Eduardo Fortunato

Abstract The resilient response of the ballast layer is a key aspect for stress–strain behavior of rail track lines. This paper presents part of an extensive research that has been evaluating the possibility of using, with operational benefits, Inert Steel Aggregates for Construction (ISAC) as heavy haul railroad ballast material. Stress–strain analyses were performed by finite element method (FEM) whose pseudo-elastic parameters for nonlinear constitutive laws were obtained from resilient modulus tests by Method B from European Standard EN 13,286-7 (CEN: Unbound and hydraulically bound mixtures—Part 7: cyclic load triaxial test for unbound mixtures. EN 13,286–7, Brussels (2004) [CEN (European Committee for Standardization) (2004) Unbound and hydraulically bound mixtures—Part 7: cyclic load triaxial test for unbound mixtures. EN 13286-7, Brussels]) for 'higher stress levels' carried out under scaled down ballast specimens in a ratio of 1:2.5 from ballast standard AREMA N. 24 (AREMA, Manual for railway engineering, vol I–IV. Lanham (2015) [AREMA (American Railway Engineering Maintenance-of-way Association) (2015) Manual for railway engineering, vol I–IV. Lanham, USA]). The numerical simulations were carried out at two loading levels (32.5 and 40 t/axle) increased by dynamic impact coefficient of 1.4. The results showed that the structure with ISAC ballast has lower levels of vertical displacements and moments on the rails and was able to concentrate more stress in the ballast layer decreasing slightly the stress level on the top of platform in comparison with what was observed for the structure with a well-known-granite ballast, commonly used in rail track lines around the world.

Keywords Steel slag ballast · Resilient modulus · Numerical simulations

B. G. Delgado (✉) · A. Viana da Fonseca
CONSTRUCT-GEO, Faculty of Engineering, University of Porto, Rua Dr. Roberto Frias S/N, Porto, Portugal
e-mail: up201502655@fe.up.pt

A. Viana da Fonseca
e-mail: viana@fe.up.pt

E. Fortunato
National Laboratory for Civil Engineering, Av. do Brasil 101, Lisboa, Portugal
e-mail: efortunato@lnec.pt

E. Tutumluer et al. (eds.), *Advances in Transportation Geotechnics IV*,
Lecture Notes in Civil Engineering 165,
https://doi.org/10.1007/978-3-030-77234-5_16

1 Introduction

The circular economy concept has driven the use of industrial by-products in several construction industry applications. Some researchers indicate that steel slags can be used, for example, in bound and unbound granular layers for transport substructures, provided that steel slag is previously stabilized to ensure its chemical and environmental stability [3, 4]. Regarding the possibility of using steel slag as railway ballast material, there are interesting studies available, but most focus is on evaluating this material just from environmental point of view, its electrical resistance or mechanical properties based on index parameters expressed in ballast specifications. This has included correlations with Los Angeles and micro-Deval tests results, or even based on particle crushing strength test results [5, 6]. However, few studies have been carried out to evaluate this material under loading and boundary conditions compatible with the application in question, especially regarding the high cyclic loading provided by passage of heavy haul trains.

In Portugal, for example, the aggregate from electrical arc furnace steel slag, after processing by steel companies, is classified as an inert aggregate, in terms of expansibility and environmental issues, having given rise to the trade denomination 'Inert Steel Aggregate for Construction (ISAC)' [4]. In the medium term, it is estimated that in Portugal, approximately 400×10^3 tonnes per year of steel slag will be produced [4], which, if used as ballast material, will allow to the construction of approximately 250 km of railway tracks per year.

Nowadays, a target for the main heavy haul freight rail companies in the world is to increase the freight capacity from about 25–32.5 to 40 tonnes per axle, sometimes under extreme weather conditions, such as in Brazilian Amazon region [7]. In Brazil, four heavy haul railway lines account for 82% of the total demand for freight railway transport. The ballast layer of these railway tracks uses natural crushed rocks, mainly granite, basalt and gneiss, with particle size distribution (PSD) curve framed in the standard gradation AREMA N. 24 [2].

Recent laboratory studies have shown that under axle loads of 40 tonnes, the ISAC ballast presented superior performance compared to traditional granite aggregate ballast with regard to long-term plastic behavior [7] due to, possibly, the highest angularity and crushing strength of its particles [8].

Thus, an extensive study has been carried out at Laboratory of Geotechnics (LabGEO) of the Faculty of Engineering of the University of Porto (FEUP) in partnership with the National Laboratory for Civil Engineering (LNEC) to evaluate the possibility to apply ISAC as railway ballast material in terms of stress–strain behavior under heavy cyclic loading conditions. Therefore, resilient modulus tests were carried out to obtain pseudo-elastic parameters aiming to simulate the railway track response from nonlinear elastic constitutive laws using a numerical solution.

2 Laboratory Tests

2.1 Overview

In order to maintain the specimen representativeness in triaxial tests, several researchers have recommended that the ratio between the maximum particle size and the diameter of specimen needs to be about 1/6. This ratio is also specified by American Standard ASTM D5311 [9] for soils. However, some results shown that a ratio of 1/5 has lead to good results [10]. Moreover, Bishop and Green [11] recommend that the ratio between height (H) and diameter of sample (D) should approach two, being this recommendation adopted almost universally in geotechnical laboratories. These restrictions imply the need of 'extra-large' (and expensive) triaxial apparatus for ballast laboratory studies [12, 13].

With the purpose to perform triaxial tests with granular materials at lower costs, Lowe [14] proposed to carry out tests with the material on scaled down specimens by parallel gradation technique, where a smaller PSD curve, but composed of the same material, can be used in triaxial cells (large but not 'extra-large') if the scaled PSD curve is parallel to the full-scale PSD curve of the material.

The scale reduction techniques of triaxial specimens to evaluate the geomaterials mechanical behavior are not consensual among the researchers. However, regarding deformability parameters, Sevi and Ge [15] conducted studies that pointed to the possibility of carrying out triaxial tests with scaled down specimens by parallel gradation technique, when the characteristics of constituting particles are similar (e.g., size, shape, surface roughness, particle crushing strength, resistance to attrition). This would ensure that the material at the same compaction level (relative density) would attain similar physical indices on full or reduced scale.

Rosa [16] correlated resilient modulus values obtained from full-scale ballast against values obtained from scaled down ballast. Ballast materials with similar particles morphology were used, both full and reduced scale, for different genesis and PSD curves, and a good correlation between modulus values were found, concluding favorably to the use of resilient ballast parameters from scaled down specimens for stress–strain analysis, since the modulus values either full-scale or scaled down had the same order of magnitude and also because the stress distribution is not so sensitive to small resilient modulus values variations.

For the studies in this paper, scaled down ballast specimens were used, obtained by parallel gradation technique in a ratio of 1:2.5 from the full-scale ballast standard AREMA N. 24 (Fig. 1a). This scaling down ratio was established as the minimum necessary to meet the 1/5 restriction between the maximum particle size and the diameter of specimen, as specimens of 150 mm diameter and 300 mm height were used. These specimens were molded by vacuum (usual procedure for non-cohesive granular materials) which was only possible due to completely dry ballast specimens. After molding, the specimens were instrumented with three axial linear variable differential transducers (LVDTs), at 120° from each other, fixed along the entire

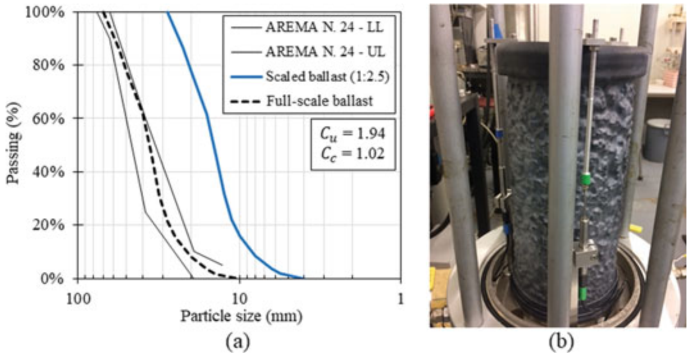

Fig. 1 **a** Particle size distribution of scaled ballast from AREMA N. 24 limits; and **b** example of scaled ballast specimen with LVDTs

height of the specimens; for this, a screw system was fixed at triaxial cell base and at top-cap of specimens tested (Fig. 1b).

The tests to determine the resilient modulus were carried out according to the method B (constant confining pressure) by European Standard EN 13,286-7 [1], applying the 'higher stress level' protocol. Figure 2 shows the stress paths, in the $p' - q$ plane, applied during triaxial tests to define the resilient modulus values of the studied materials, in which 100 cycles per path are applied (resilient modulus test). More details about the triaxial apparatus can be seen in Delgado et al. [7]. The tests strictly follow the standard procedure, after specimen conditioning with 20,000 cycles of deviatoric stress application with 340 kPa and a constant confining pressure of 70 kPa.

Fig. 2 Cyclic stress paths for resilient modulus test in the high stress level (HSL) with constant confining pressure (method B by EN 13,286-7 [1])

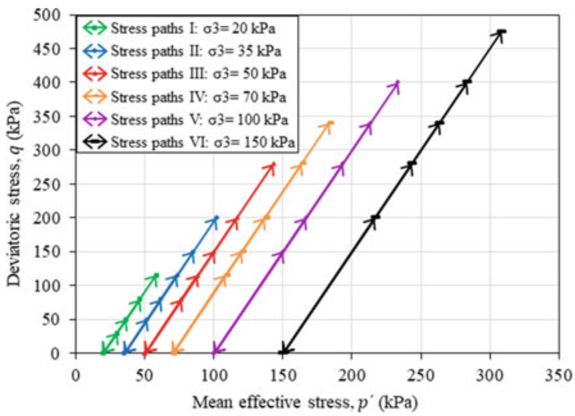

2.2 Resilient Parameters

Figure 3 shows the resilient modulus values obtained by laboratory triaxial tests. The results are presented both against confining pressure and cyclic deviatoric stress (q_{cyc}). For all applied stress paths, it can be seen that the ISAC presented higher values of resilient modulus than the granite aggregate. It is important to note that in both materials, as expected for non-cohesive granular materials, the values of resilient modulus were more sensitive to variation of the confining pressure than to variation of the deviatoric stress, at least for the low-to-moderate stress ratios (q_{cyc}/p').

It should be noted that all resilient modulus tests were considered satisfactory, since the accumulated permanent deformation during the tests was less than 0.2%.

The stiffness parameters obtained by regression analyses for the models of resilient behavior that take into account the variation of the resilient modulus (RM) against the confining pressure and against the cyclic deviatoric stress, as well as the model that takes into account the variation of the RM against the first invariant of stresses (θ), are shown in Table 1, for the resilient modulus tests performed. For triaxial tests under axisymmetric stress conditions, we have:

$$\theta = \sigma_1 + 2.\sigma_3 = q_{cyc} + 3.\sigma_3 \tag{1}$$

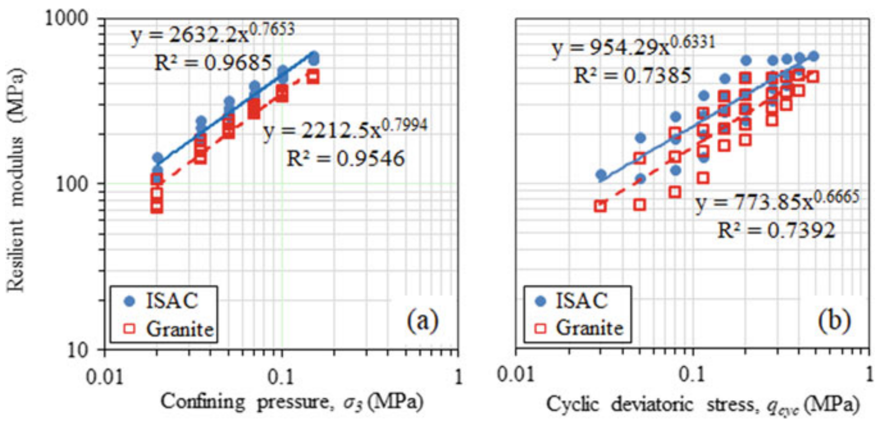

Fig. 3 Variation of resilient modulus for the ballast materials against: **a** confining pressure and **b** cyclic deviatoric stress

Table 1 Resilient parameters of nonlinear elastic ballast models

Material	Model		
	$\mathrm{RM} = K_1\sigma_3^{K_2}$	$\mathrm{RM} = K_1 q_{cyc}^{K_2}$	$\mathrm{RM} = K_1'\theta^{K_2'}$
ISAC	K_1=2632.2 K_2=0.7653 ($R^2 = 0.9685$)	K_1=954.3 K_2=0.6331 ($R^2 = 0.7385$)	K_1'=1692.4 $K_2' = 0.7986$ ($R^2 = 0.9531$)
Granite	K_1=2212.5 K_2=0.7994 ($R^2 = 0.9546$)	K_1=773.9 K_2=0.6665 ($R^2 = 0.7392$)	K_1'=1368.1 K_2'=0.8269 ($R^2 = 0.9466$)

Note $q = \sigma_1 - \sigma_3$, being σ_1 the major principal stress (vertical cyclic loading) and σ_3 is the minor principal stress (usually the constant confining pressure in the triaxial cell)

3 Numerical Simulations

3.1 Finite Element Analyses

Four scenarios were simulated: (i) Scenario 1–32.5 t/axle loading with ISAC ballast; (ii) Scenario 2–32.5 t/axle loading with granite aggregate ballast; (iii) Scenario 3–40 t/axle loading with ISAC ballast; and (iv) Scenario 4–40 t/axle loading with granite aggregate ballast. The *SysTrain* (version 1.63) software was used, which was developed at the Military Institute of Engineering (IME) from Brazil. The software models both superstructure (rails, sleepers and fastening system) and substructure (ballast, sub-ballast and subgrade) by finite element method (FEM) and presents as major attractions for users: (i) a 3D graphical interface based on the *MS-Windows*® platform; (ii) parametric modeling from a predefined rail track geometry; (iii) constitutive models and some materials with parameters already pre-registered, with the possibility, however, of alteration or inclusion of new models and/or materials; and (iv) a relatively fast and reliable stress–strain analysis in elastic regime (under static loading).

Silva Filho [17] provides a detailed description of the discretization, parameterization, numerical integration and convergence methods adopted by *SysTrain*. He was a member of the software development team and reports also that the software has undergone several calibration processes, both by field instrumentation and by comparison with another numerical model (*ANSYS*® v.15), ensuring analyzes with a good reliability level.

The software is three-dimensional and allows several possibilities regarding the number of sleepers, number of substructure layers, types and position of loading (on the symmetry axis of sleepers or on the gap between them), substructure layers geometry, etc. About the constitutive models for the rail track components, both superstructure and substructure, the software has nine predefined models.

The boundary conditions define a lower rigid boundary and null displacements in the normal direction to the model's vertical boundary planes.

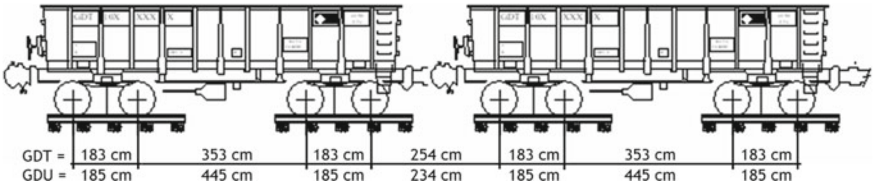

Fig. 4 Scheme of two consecutive gondola wagons (GDT/GDU—not to scale) [18]

The most severe condition for stress–strain analysis of heavy haul rail tracks is given by the bogies between adjacent wagons [18]. Thus, the loading for simulations was defined as being imposed by two bogies between couplings of two consecutive gondola wagons (GDT type for 32.5 t/axle loading and GDU type for 40 t/axle loading) (Fig. 4), applied to a structure with nineteen sleepers (same spacing). More details about these wagons can be seen in Santos et al. [19].

Figure 5 shows a cross section of the rail track structure, with dimensions of the components and layers used to the numerical simulations. Figure 6a shows the load distribution applied by GDU wagons used to simulate 40 t/axle loading (the loads

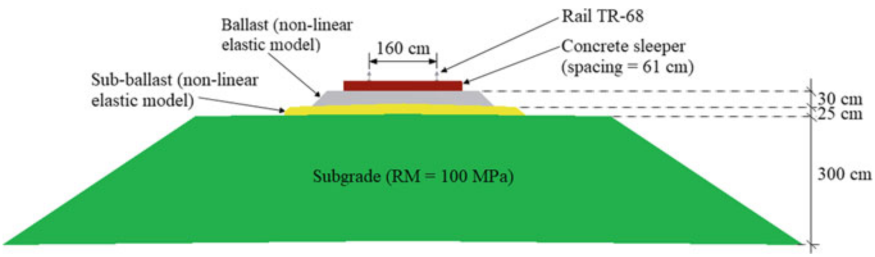

Fig. 5 Cross section with simulated rail track structure (not to scale)

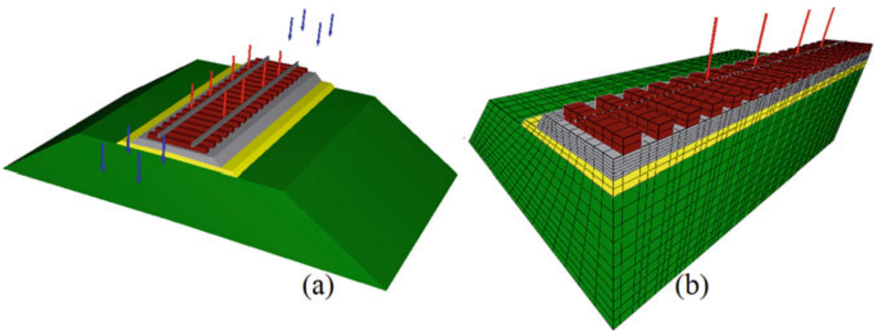

Fig. 6 3D rail track structure used to FEM simulations with GDU wagons: **a** geometric and load distribution model (red arrows represent the wheels loading the model; the blue arrows represent only geometric positions of the extreme wheels of wagons) and **b** finite element mesh

corresponding to the two extreme axles, blue vectors, were not considered in the simulations). Figure 6b shows the three-dimensional finite element mesh employed in the analysis for this loading level, which is transversely symmetrical with respect to a vertical axis located midway between rails.

Considering that the *SysTrain* software only simulates static loading under the structure and assuming a dynamic coefficient of 1.4, estimated by empirical equations [2], the 32.5 t/axle loading was converted into a GDT wagon with a total gross weight of 182 tonnes. Similarly, the 40 t/axle loading was increased with the same impact factor, resulting in a total gross weight of 224 tonnes per GDU wagon.

The parameters used to the simulations are presented in Table 2. For the ballast, the parameters were obtained by linear regression taking into account the variation of the resilient modulus against the confining pressure, due to the good fit of this model for studied materials. For the sub-ballast, the parameters were obtained from Delgado [18]. The other parameters were obtained from the software library.

In addition, four additional simulations were carried out, considering the same load levels, materials and boundary conditions, but with a unit load applied to the vertical centerline of a central sleeper under a structure with nine sleepers. This loading framework is the critical condition for sleeper–ballast contact stress.

3.2 Results

Figure 7 shows the 3D deformed meshes with the node vertical displacements for the four simulated scenarios.

For all carried out simulations, the negative result values indicate compressive stresses and downward displacements and the positive result values indicate tensile stresses and upward displacements.

As expected, the maximum displacements occur in the regions immediately below the load application points. For both studied materials, both for the 32.5 t/axle (scenarios 1 and 2) and the 40 t/axle (scenarios 3 and 4), the maximum displacements on the rail top level were similar for both materials under the same loading level.

For axle load of 32.5 tonnes, the maximum displacements obtained were below the tolerance limit recommended by AREMA [2], which is 6.35 mm, but slightly lower for ISAC (5.87 mm) in comparison to the granite aggregate ballast (6.05 mm), implying that the rail track structure with ISAC ballast is stiffer for this loading level.

However, for 40 t/axle loading the maximum displacements obtained were already above the tolerance limit [2]. Nevertheless, the values were again slightly lower for the ISAC (7.41 mm) in comparison to the granite aggregate (7.64 mm), showing again the higher stiffness of the rail track structure with ISAC ballast also for this loading level, as can be compared in Fig. 8 for the four simulated scenarios.

The maximum vertical stress values in the ballast layer for both studied materials were reached, as expected, at the base of sleepers. Figure 9 shows sleeper–ballast interface contact stress for all additional simulated scenarios, in a semi-cross section

Table 2 Material parameters adopted in FEM analysis

Rail track component	Parameter	Value			
		Scenario 1	Scenario 2	Scenario 3	Scenario 4
Rails	Density (kg/m^3)	7850	7850	7850	7850
	Elastic modulus (Pa)	210×10^9	210×10^9	210×10^9	210×10^9
	Poisson's ratio	0.30	0.30	0.30	0.30
Sleepers	Density (kg/m^3)	2400	2400	2400	2400
	Elastic modulus (Pa)	32×10^9	32×10^9	32×10^9	32×10^9
	Poisson's ratio	0.25	0.25	0.25	0.25
Fastenings	Spring stf. K_x (N/m)	7×10^6	7×10^6	7×10^6	7×10^6
	Spring stf. K_y (N/m)	7×10^6	7×10^6	7×10^6	7×10^6
	Spring stf. K_z T (N/m)	70×10^6	70×10^6	70×10^6	70×10^6
	Spring stf. K_z C (N/m)	70×10^6	70×10^6	70×10^6	70×10^6
Ballast	Bulk density (kg/m^3)	1800	1550	1800	1550
	Coefficient K_1'	67,378.12	35,357.64	67,378.12	35,357.64
	Coefficient K_2'	0.7653	0.7994	0.7653	0.7994
	σ_3 minimum (Pa)	20.7×10^3	20.7×10^3	20.7×10^3	20.7×10^3
	σ_3 maximum (Pa)	137.9×10^3	137.9×10^3	137.9×10^3	137.9×10^3
	Poisson's ratio	0.20	0.20	0.20	0.20
Sub-ballast	Bulk density (kg/m^3)	1730	1730	1730	1730
	Coefficient K_1'	131.22×10^6	131.22×10^6	131.22×10^6	131.22×10^6
	Coefficient K_2'	− 0.232	− 0.232	− 0.232	− 0.232
	σ_d minimum (Pa)	1×10^3	1×10^3	1×10^3	1×10^3
	σ_d maximum (Pa)	206×10^3	206×10^3	206×10^3	206×10^3
	Poisson's ratio	0.40	0.40	0.40	0.40
Subgrade	Bulk density (kg/m^3)	1800	1800	1800	1800
	Coefficient K_1'	100×10^6	100×10^6	100×10^6	100×10^6

(continued)

Table 2 (continued)

Rail track component	Parameter	Value			
		Scenario 1	Scenario 2	Scenario 3	Scenario 4
	Poisson's ratio	0.40	0.40	0.40	0.40

Notes stf. Stiffness, *T* Tensile, *C* Compression
Units expressed in the International System of Units (*SI*) except Spring St.
For ballast layer, the coefficient K_1' was obtained from experimental parameter K_1 (RM test). Considering the 'Granular Resilient 1' model from the software, this coefficient is given by: $K_1' = K_1.10^{\alpha(1-K_2)}$ and $K_2' = K_2$, being for K_1 given in MPa: $\alpha = 6$.

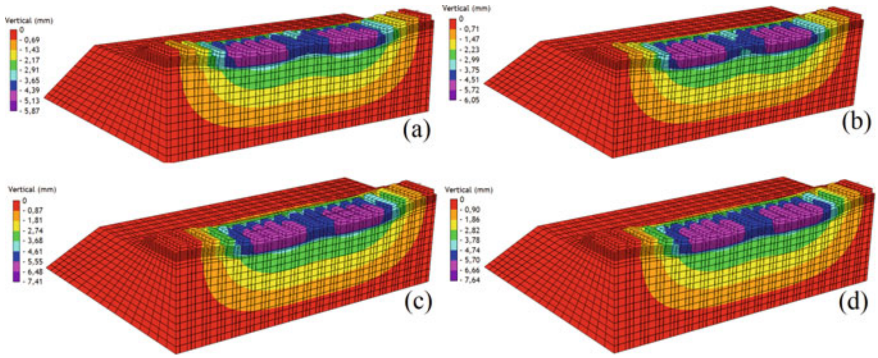

Fig. 7 Total vertical displacements of the rail track structure: **a** Scenario 1 (ISAC—32.5 t/axle), **b** Scenario 2 (Granite—32.5 t/axle), **c** Scenario 3 (ISAC—40 t/axle) and **d** Scenario 4 (Granite—40 t/axle)

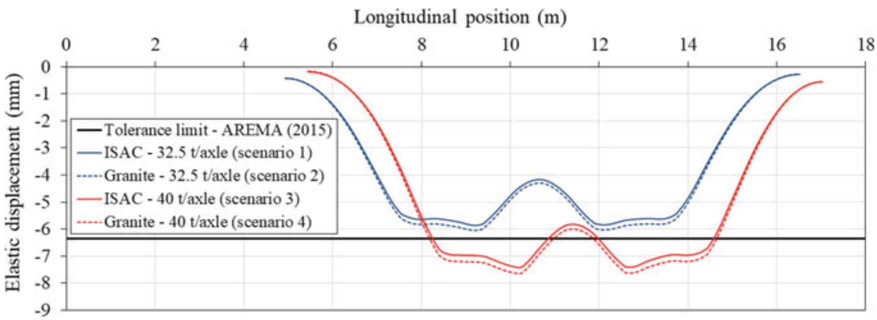

Fig. 8 Vertical elastic displacements of rail track on the rail top level

(*Y*-axis) of a sleeper, for both GDT (32.5 t/axle) and GDU (40 t/axle) wagons, from the centerline of the loaded sleeper (critical condition).

It was observed that in the rail track structure with ISAC ballast, the contact stress with the sleeper was higher than to the granite aggregate ballast structure, mainly

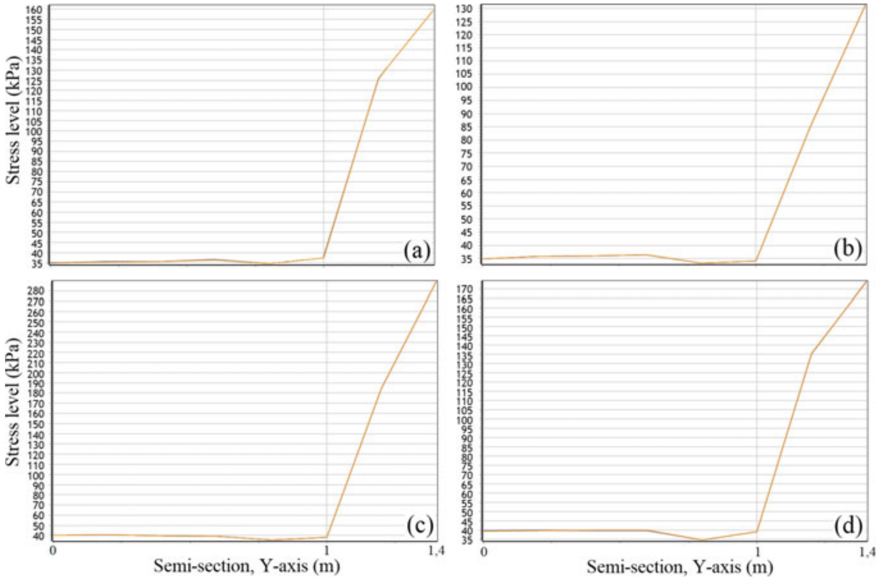

Fig. 9 Sleeper–ballast contact stress: **a** Scenario 1 (ISAC—32.5 t/axle), **b** Scenario 2 (Granite—32.5 t/axle), **c** Scenario 3 (ISAC—40 t/axle) and **d** Scenario 4 (Granite—40 t/axle)

at sleeper extremity. In the sleeper centerline, both materials showed very similar contact stress and not much higher when loading increased from 32.5 to 40 t/axle. The maximum stress values in the sleeper–ballast contact for all simulated scenarios were observed at the sleeper extremity, being 159 kPa for ISAC and 133 kPa for granitic aggregate, considering axle load of 32.5 tonnes; and 288 kPa for ISAC and 174 kPa for granite aggregate when 40 t/axle loading was applied. For all simulated scenarios, the maximum stress values at the sleeper–ballast contact are well below the most restrictive limit recommended by AREMA [2], which is 448 kPa.

Table 3 summarizes the vertical compression stress levels obtained in each layer of the rail track for all simulated scenarios

Regarding the vertical stress level transferred to the sub-ballast, it was found that for 32.5 t/axle loading the maximum value obtained for the rail track structure with ISAC ballast (scenario 1) was slightly higher than for the structure with granite aggregate ballast (scenario 2). However, probably due to the higher stiffness mobilized in

Table 3 Maximum vertical tress levels on top of substructure layers

Top of layer	Maximum vertical stress (kPa)			
	Scenario 1	Scenario 2	Scenario 3	Scenario 4
Ballast	159	133	288	174
Sub-ballast	121	117	133	139
Subgrade	70	73	110	120

the structure with ISAC ballast when the axle load level has increased to 40 tonnes, the maximum value obtained for the rail track structure with ISAC ballast (scenario 3) was slightly lower than the obtained for the structure with granite aggregate ballast (scenario 4). Nevertheless, the materials showed very close vertical stress transferred to the sub-ballast, and both materials were able to transfer to this layer stress values below the 172 kPa limit suggested by AREMA [2] as limit stress in platform.

On top of the subgrade, the maximum vertical stresses obtained were also very close considering the different materials. However, for 40 t/axle loading relatively high stress values were observed. Thus, for this loading level some rail track design approaches, such as sleepers spacing reduction or sub-ballast thickness increasing, can be useful to control the induced subgrade stress, improving the rail track performance.

About the maximum bending moment on the rail top level, for axle load of 32.5 tonnes the obtained value for the ISAC ballast structure was 46.05 kN m, slightly lower than for the granite aggregate ballast structure whose was 46.74 kN m. Both values are below the maximum allowable for the rails considered in the analyses (TR-68), which is 67.98 kN m. Considering the axle load of 40 tonnes, the value obtained for the ISAC ballast structure was 58.66 kN m, still lower than those verified when simulating the granite ballast structure (59.46 kN m), both again below allowable value.

4 Conclusions

Although the performance of both materials is similar, when considering 40 t/axle loading the rail track structure with ISAC ballast performs better than the granite aggregate ballast according as its higher stiffness can decrease the rail track platform stress.

The fact that none of the rail track structures met the maximum vertical displacement criterion for axle load of 40 tonnes [2] does not make the application of this load level permanently unfeasible, as this limit of 6.35 mm, which was not defined from rail tracks with operations under this loading level, can be reviewed. Thus, further studies are needed to assess of long-term effects on both rail track and vehicle components. In addition, both materials met the other design criteria for this loading level.

Acknowledgements The first author's PhD fellowship [201518/2015-5] was supported by National Council for Scientific and Technological Development (CNPq) from Brazil. Special thanks to 'Siderurgia Nacional da Maia' for providing the ISAC material and to the IME for the *SysTrain* software license. Part of the work was conducted in the framework of the TC202 National Committee of the Portuguese Geotechnical Society (SPG) 'Transportation Geotechnics', in association with the International Society for Soil Mechanics and Geotechnical Engineering (ISSMGE).

References

1. CEN (European Committee for Standardization) (2004) Unbound and hydraulically bound mixtures—Part 7: cyclic load triaxial test for unbound mixtures. EN 13286-7, Brussels
2. AREMA (American Railway Engineering Maintenance-of-way Association) (2015) Manual for railway engineering, vol I–IV. Lanham, USA
3. Mathur S, Soni S, Murty A (1999) Utilization of industrial wastes in low-volume roads. Transp Res Rec 1652(1):246–256
4. Gomes A, Roque A, Ferreira S, Fortunato E (2012) Case study to promote the use of industrial byproducts: the relevance of performance tests. J ASTM Int 9(2):1–18
5. Morata M, Saborido C (2016) Slag aggregates with enhanced performance for railway track bed layers. In: Proceedings of the third international conference on railway technology: research, development and maintenance, pp 1–17. Cagliari, Italy
6. Kuo C, Lin C (2017) Engineering performance of steel slag as railway ballast. In: Proceedings bearing capacity of roads, railways and airfields, pp 1859–1864. Athens, Greece
7. Delgado B, Viana da Fonseca A, Fortunato E, Maia P (2019) Mechanical behavior of inert steel slag ballast for heavy haul rail track: laboratory evaluation. Transport Geotech 20(100243): 1–10
8. Delgado B, Viana da Fonseca A, Fortunato E, Motta L (2019) Particle morphology's influence on the rail ballast behaviour of a steel slag aggregate. Environ Geotech https://doi.org/10.1680/jenge.18.00203
9. ASTM (American Society for Testing Materials) (2004) Standard test method for load cyclic triaxial strength of soil. D5311, USA
10. Skoglund K (2002) A study of some factors in mechanistic railway track design. PhD Thesis, Norwegian University of Science and Technology, Norway
11. Bishop A, Green G (1965) The influence of end restraint on the compression strength of a cohesionless soil. Géotechnique 15(1):243–266
12. Fortunato E, Pinelo A, Matos Fernandes M (2010) Characterization of the fouled ballast layer in the substructure of a 19th century railway track under renewal. Soils Found 50(1):55–62
13. Indraratna B, Salim W, Rujikiatkamjorn C (2011) Advanced rail geotechnology—ballasted track. Taylor & Francis Group, London
14. Lowe J (1964) Shear strength of coarse embankment dam materials. In: Proceedings of 8th Congress on Large Dams, Transactions, Vol. III, International Commission on Large Dams, pp 745–761. Paris, France
15. Sevi A, Ge L (2012) Cyclic behaviors of railroad ballast within the parallel gradation scaling framework. J Mater Civ Eng ASCE 24:797–804
16. Rosa A (2019) Effect of granulometry and lithology on ballast behavior by laboratory and computational analysis. Master thesis, Federal University of Rio de Janeiro, Brazil (in Portuguese)
17. Silva Filho J (2018) Contribution to development of a mechanistic-empirical method for rail track design focusing tropical soil substructures. PhD thesis, Military Institute of Engineering, Brazil (in Portuguese)
18. Delgado B (2012) Deformability assessment of a tropical soil from western Maranhão state as sub-ballast material for Carajás Railroad. Master thesis, Federal University of Ouro Preto, Brazil (in Portuguese)
19. Santos G, Barbosa R, Shu X, Urban C, Joy R (2014) Characterization and modelling of a new heavy axle load freight wagon for wheel rail wear prediction. J Mechan Eng Technol 2(3):17–28